

# Additive Differential Double Pulse Voltammetry Applied to the Study of Multistep Electron Transfer Reactions with Microelectrodes of Different Geometries

A. Molina<sup>1\*</sup>, J. Gonzalez<sup>1</sup>, E. Laborda<sup>1,2</sup>, R. G. Compton<sup>2,\*</sup>

<sup>1</sup> Departamento de Química Física, Universidad de Murcia, 30100 Murcia, Spain

<sup>2</sup> Department of Chemistry, Physical and Theoretical Chemistry Laboratory, Oxford University, South Parks Road, Oxford OX1 3QZ, United Kingdom

\*E-mail: [amolina@um.es](mailto:amolina@um.es); [richard.compton@chem.ox.ac.uk](mailto:richard.compton@chem.ox.ac.uk)

Received: 7 May 2012 / Accepted: 4 June 2012 / Published: 1 July 2012

---

Additive differential double pulse voltammetry (ADDPV) is applied to the study of reversible multistep electron transfers at microelectrodes of different geometries, including discs, (hemi)spheres, bands and cylinders. Analytical expressions are deduced for arbitrary numbers of electrons transferred and for any difference between the formal potentials of the different redox couples. ADDPV curves show two or more peaks and one or more crossing potentials depending on the number of steps, the difference between the formal potentials and the pulse amplitude employed. The variation of the voltammograms with the electrode size and shape, the pulse amplitude and the difference between formal potentials is described. The optimal extraction of the values of the formal potentials from the ADDPV signal is also described. In this context, the use of the crossing potentials is particularly valuable since they can be measured with better accuracy than peak parameters and they are independent of experimental variables like the electrode geometry and size.

---

**Keywords:** Multistep electron transfer; Additive differential double pulse voltammetry; Disc microelectrodes; Band microelectrodes; Cylindrical microelectrodes

## 1. INTRODUCTION

The electrochemistry of numerous species includes successive electron transfer steps (see scheme (1)). This is the case for many organic and organometallic compounds [1-4], biomolecules (nucleic acids, dopamine, ascorbic acid, etc.) [5-7] as well as nanoparticles [8]. The electrochemical response depends on the properties of the different oxidation states in solution and hence on the interactions existing between the different redox centers and with the surrounding medium [9-13]. Unfortunately, in many cases the analysis of the voltammograms is not straightforward due to the

overlapping of signals corresponding to different steps. Thus, the development of theoretical and practical tools to facilitate the study of these redox systems has received a lot of attention [14-24].

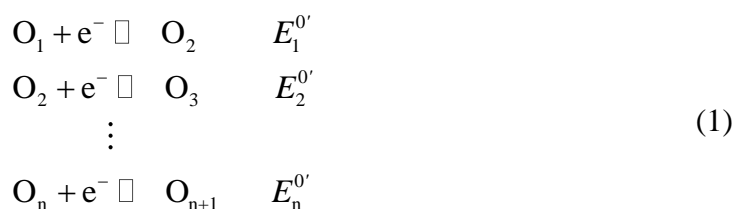
In previous works we contributed to the above development by deriving simple, analytical expressions for the study of multistep electron transfer processes via cyclic voltammetry (CV), square wave voltammetry (SWV) and other differential techniques on disc and (hemi)spherical microelectrodes [25-27]. The results obtained showed the convenience of using differential techniques (like SWV and differential staircase voltammetry) since the response is always peak-shaped with better definition and symmetry than cyclic voltammograms, especially when very small electrodes are employed.

In the present paper we go further by considering the application of additive differential double pulse voltammetry (ADDPV) [28] to the study of reversible multistep electrode reactions, regardless of the number of steps and the differences between the formal potentials. In ADDPV two differential double pulse voltammetry (DDPV) experiments are performed with the same absolute value of the pulse amplitude ( $\Delta E$ ) but opposite signs as shown in Figure 1.A. The ADDPV signal (see Figure 1.B) results from adding the two differential voltammograms recorded. Depending on the number of steps and the difference between the formal potentials, ADDPV voltammograms can show two or more peaks and one or more crossing points corresponding to the intersection of the current with the potential axis. This offers a very valuable procedure for the determination of the formal potentials since, besides its simplicity, the crossing potentials can often be measured experimentally with better precision than the peak potentials and widths in other differential techniques. Moreover, their value is independent of the electrode geometry and it is not affected by uncertainties in experimental variables such as the electrode size, the concentration of electroactive species and the diffusion coefficient. As a differential pulse method the ADDPV technique also leads to a significant reduction of the effects due to charging and background currents. Therefore, the voltammograms obtained are well-defined which is very convenient for the quantitative analysis of the system.

Besides the two most usual electrode geometries (microdisc and microhemispheres), the theory presented here is also valid for cylinder and band electrodes of any size. The results are applied to the EE mechanism, analyzing the influences of the difference between formal potentials, the electrode size and geometry, and the pulse amplitude on the ADDPV voltammograms. Procedures for the extraction of the formal potentials are given for the different situations that can be found depending on the magnitude of the difference between the formal potentials.

## 2. THEORY

Let us consider the reduction of a molecule present in solution with  $n+1$  possible oxidation states  $O_1, O_2, \dots, O_{n+1}$  (i.e., a multi-E mechanism):



where  $E_i^{0'}$  ( $i=1, 2, \dots, n$ ) are the formal potentials of each electron transfer. Comproportionation reactions have been demonstrated not to affect the voltammetric response under the conditions considered in this work, that is, when diffusion is the only mass transport mechanism, the value of the diffusion coefficient is the same for all the species  $O_i$ , the electron transfers are reversible and the absence of any other chemical reaction [16,19,29].

In the following, we will study the electrochemical response of a process following the scheme (1) when applying two consecutive potential pulses  $E_1$  and  $E_2$  with lengths  $t_1$  and  $t_2$ , respectively, to an electrode with the characteristic dimension  $r_0$ . The most commonly used electrode geometries will be considered, that is, disc ( $r_0 = r_d$ ), spherical ( $r_0 = r_s$ ), cylinder ( $r_0 = r_c$ ) and band ( $r_0 = w$ ) electrodes. By following the procedure indicated in references [25-27], the following expressions corresponding to the currents of the first and second potential steps,  $I^{(1)}$  and  $I^{(2)}$  respectively, are obtained:

$$I^{(1)} = FADc_{O_i}^* g(t_1, r_0) \left( \sum_{i=1}^n (n-i+1) f_{O_i}(E_1) \right) \tag{2}$$

$$I^{(2)} = I^{(1)}(t_1 + t_2) + FADc_{O_i}^* g(t_2, r_0) \left( \sum_{i=1}^n (n-i+1) f_{O_i}(E_2) \right) \tag{3}$$

where the time function  $g(t, r_0)$  is dependent on the electrode size and shape (see Table 1):

**Table 1.** Expressions for the function  $g(t, r_0)$  for the main electrode geometries.  $r_0$  is the characteristic dimension of the electrode.

Electrode	Function $g(t, r_0)$
Planar	$\frac{1}{\sqrt{\pi Dt}}$
Spherical (radius $r_s$ ) [25, 35]	$\frac{1}{\sqrt{\pi Dt}} + \frac{1}{r_s}$
Cylindrical (radius $r_c$ , length l) [33]	$\frac{e^{-0.1(\pi Dt)^{1/2}/r_c}}{\sqrt{\pi Dt}} + \frac{1}{r_c} \frac{1}{\ln \left( 5.2945 + 1.4986 \frac{\sqrt{Dt}}{r_c} \right)}$
Band (height w, length l) [32]	$\frac{1}{w} + \frac{1}{\sqrt{\pi Dt}}$ for $Dt / w^2 < 0.4$ $0.25 \sqrt{\frac{\pi}{Dt}} e^{-0.4(\pi Dt)^{1/2}/w} + \frac{1}{w} \frac{\pi}{\ln \left( 5.2945 + 5.9944 \frac{\sqrt{Dt}}{w} \right)}$ for $Dt / w^2 \geq 0.4$
Disc (radius $r_d$ ) [31]	$\frac{4}{\pi r_d} \left( 0.7854 + 0.44315 \frac{r_d}{\sqrt{Dt}} + 0.2146 \exp \left( -0.39115 \frac{r_d}{\sqrt{Dt}} \right) \right)$

Note that the function  $g(t, r_0)$  of spherical electrodes is derived from the exact analytical solution [30] whereas in the case of other geometries it is obtained from the semi-empirical Shoup and Szabo equations (disc and band electrodes) [31,32] and from the Aoki equation for the cylindrical ones [33]. The accuracy of the semi-empirical expressions has been tested in previous papers [34] by comparison with numerical results, giving rise to errors below 0.5% in all the cases.

With respect to the potential function  $f_{O_i}(E_m)$  ( $m=1,2$ ), this is independent of the electrode geometry:

$$f_{O_i}(E_m) = \frac{1}{c_{O_i}^*} \left( c_{O_i}^{(m-1)}(q_{surface}) - c_{O_i}^{(m)}(q_{surface}) \right) \quad (4)$$

where  $c_{O_i}^{(m)}(q_{surface})$  is the surface concentration of species  $i$  at the  $m$ -th pulse such that  $c_{O_1}^{(0)}(q_{surface}) = c_{O_1}^*$ ,  $c_{O_{i \geq 2}}^{(0)}(q_{surface}) = 0$ , and:

$$\left. \begin{aligned} \frac{c_{O_i}^{(m)}(q_{surface})}{c_{O_i}^*} &= \frac{\prod_{j=i}^n J_j^{(m)}}{1 + \sum_{m=1}^n \left( \prod_{j=m}^n J_j^{(m)} \right)}, \quad i = 1, 2, \dots, n \\ \frac{c_{O_{n+1}}^{(m)}(q_{surface})}{c_{O_1}^*} &= \frac{c_{O_1}^*}{1 + \sum_{m=1}^n \left( \prod_{j=m}^n J_j^{(m)} \right)} \end{aligned} \right\} m=1, 2 \quad (5)$$

$$J_i^{(m)} = \exp \left( \frac{F(E_m - E_i^{0'})}{RT} \right) \quad m=1, 2 \quad (6)$$

For the particular simpler case of a two steps reduction (EE mechanism), the above equations can be written in the following simpler way:

$$I^{(1)}(t_1) = FADc_{O_1}^* g(t_1, r_0) \Omega_1 \quad (7)$$

$$I^{(2)} = I^{(1)}(t_1 + t_2) + FADc_{O_1}^* g(t_2, r_0) \Omega_2 \quad (8)$$

where:

$$\Omega_1 = \frac{J^{(1)} + 2K}{(J^{(1)})^2 + J^{(1)} + K} \quad (9)$$

$$\Omega_2 = \frac{J^{(2)} + 2K}{(J^{(2)})^2 + J^{(2)} + K} - \frac{J^{(1)} + 2K}{(J^{(1)})^2 + J^{(1)} + K} \quad (10)$$

$$K = \exp\left(\frac{F}{RT}(E_2^{0'} - E_1^{0'})\right) \tag{11}$$

$$\left. \begin{aligned} J^{(1)} &= \exp\left(\frac{F}{RT}(E_1 - E_1^{0'})\right) \\ J^{(2)} &= \exp\left(\frac{F}{RT}(E_2 - E_1^{0'})\right) \end{aligned} \right\} \tag{12}$$

2.1. Additive double differential pulse technique (ADDPV)

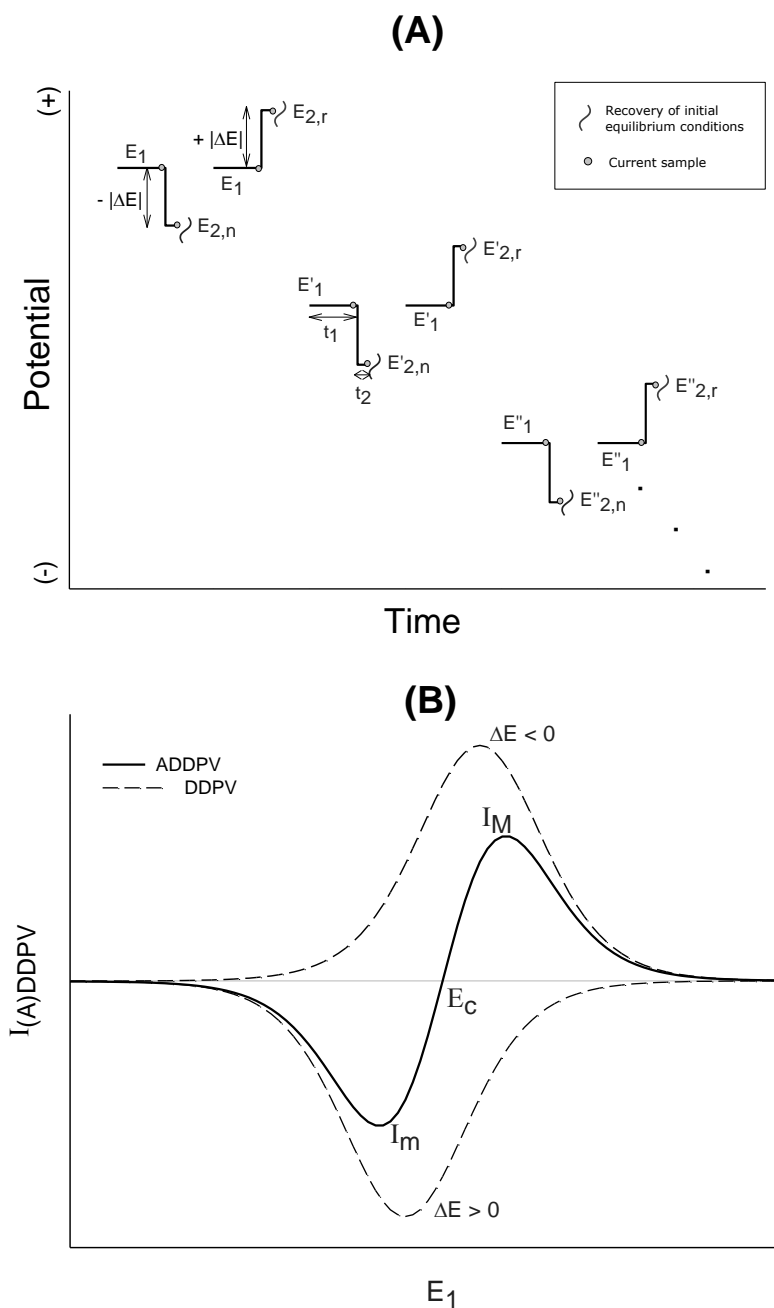


Figure 1. Additive Differential Pulse Voltammetry: (A) Potential waveform, (B) Signal.

As can be seen in Figure 1.A, in additive double differential pulse technique (ADDPV) two DDPV experiments are performed with the same absolute value of the pulse height ( $\Delta E$ ) in normal mode ( $\Delta E < 0$ ) and in reverse mode ( $\Delta E > 0$ ). The resulting DDPV curves are summed such that the ADDPV signal is given by:

$$I_{ADDPV} = \Delta I_{normal} + \Delta I_{reverse} = I_2(E_1 - |\Delta E|) + I_2(E_1 + |\Delta E|) - 2I_1(E_1) \quad (13)$$

The typical morphology of ADDPV curves for a one electron transfer (E mechanism) is shown in Figure 1.B, which can be easily characterized by the magnitude of the peaks ( $I_M, I_m$ ) and by the value of the crossing potential ( $E_c$ ).

From the solution for currents  $I^{(1)}$  and  $I^{(2)}$  given by equations (2)-(3), the additive response given by Equation (13) takes the following dimensionless form:

$$\frac{I_{ADDPV}}{I_d(t_2)} = g(t_2, r_0) \left( \sum_{i=1}^n (n-i+1) f_{O_1}(E_1 - \Delta E) \right) + g(t_2, r_0) \left( \sum_{i=1}^n (n-i+1) f_{O_1}(E_1 + \Delta E) \right) - 2 \left( \sum_{i=1}^n (n-i+1) f_{O_1}(E_1) \right) (g(t_1 + t_2, r_0) - g(t_1, r_0)) \quad (14)$$

with:

$$I_d(t_2) = FAc_{O_1}^* \frac{I}{\sqrt{\pi D t_2}} \quad (15)$$

and  $D$  being the diffusion coefficient of all the species.

For any length of the potential pulses ( $t_1, t_2$ ), the response given in Equation (14) corresponds to the normal pulse mode of this technique (Additive Double Differential Normal Pulse Voltammetry, ADDNPV). When the second pulse is much shorter than the first one,  $t_2 \ll t_1$  (with  $(t_1 / t_2) \geq 50$ ), the last term in Equation (14) can be neglected and the response can be written as:

$$\frac{I_{ADDPV}}{I_d(t_2)} = g(t_2, r_0) \left[ \left( \sum_{i=1}^n (n-i+1) f_{O_1}(E_1 - \Delta E) \right) + \left( \sum_{i=1}^n (n-i+1) f_{O_1}(E_1 + \Delta E) \right) \right] \quad (16)$$

Under these conditions the technique is known as ADDPV.

For the case of the EE mechanism, Eq. (16) with  $n = 2$  becomes into (see equations (4)-(12)):

$$\frac{I_{ADDPV}}{I_d(t_2)} = g(t_2, r_0) [\Omega_{2,n} + \Omega_{2,r}] \quad (17)$$

with  $\Omega_{2,n}$  and  $\Omega_{2,r}$  given by equation (10) with  $E_2 = E_1 - |\Delta E|$  and  $E_2 = E_1 + |\Delta E|$ , respectively. Thus, the ADDPV voltammogram has a symmetry centre for any value of the difference between the

formal potentials,  $\Delta E^0 = E_2^{0'} - E_1^{0'}$ , which corresponds to null current and a potential value given by (see below and references [28,35]):

$$E_{cc} = \frac{E_1^{0'} + E_2^{0'}}{2} \tag{18}$$

### 3. RESULTS AND DISCUSSION

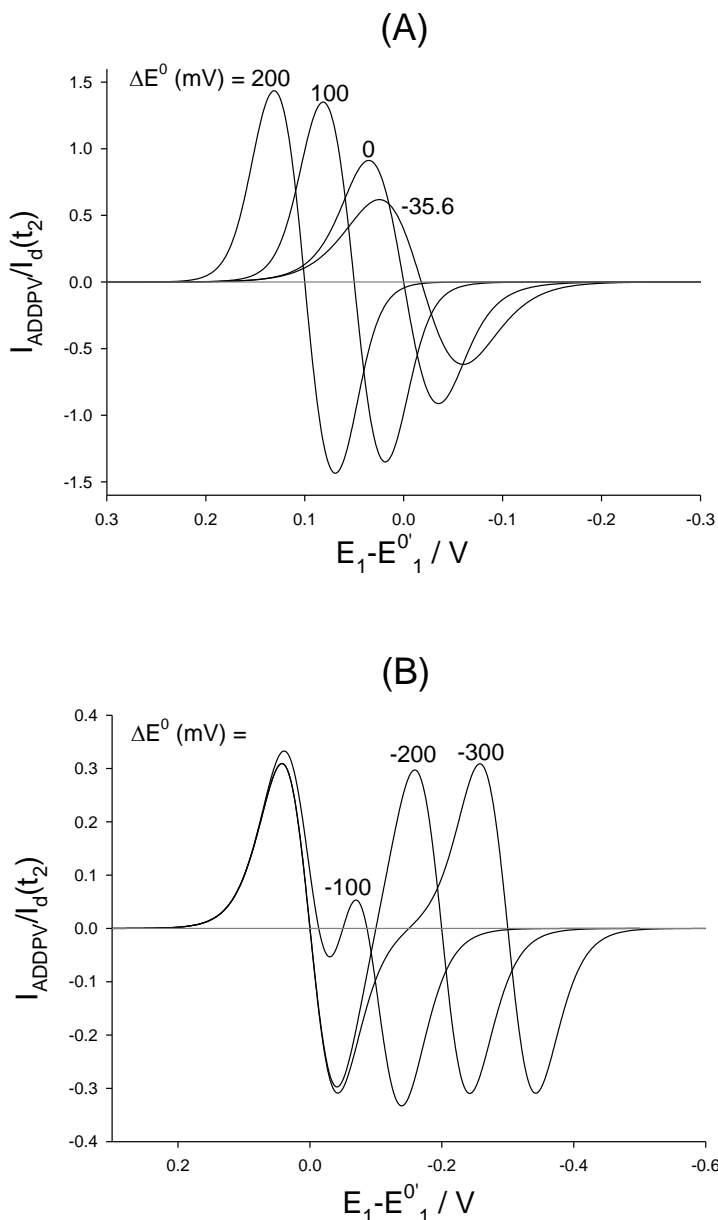


**Figure 2.** Influence of  $\Delta E^0$  on the dimensionless ADDPV curves ( $t_1/t_2 = 100$ ) for a reversible EE mechanism (Eq. (17)) at a disc electrode of radius  $r_d = 50 \mu\text{m}$ .  $|\Delta E| = 50 \text{ mV}$ ,  $t_2 = 10 \text{ ms}$ ,  $D = 10^{-5} \text{ cm}^2 \text{ s}^{-1}$ ,  $E_1^{0'} = 0 \text{ V}$ ,  $T = 298 \text{ K}$ . The values of the difference between the formal potentials of both electrochemical steps are shown on the curves.

In this section the theoretical results for the EE mechanism in ADDPV will be analyzed. Note, however, that the theory presented in section 2 is general and it can be applied to more complicated stepwise processes involving an arbitrary number of electron transfers. The temperature considered for all the calculations is 298.15 K.

Figure 2 shows the dimensionless theoretical ADDPV curves for a reversible EE mechanism (Eq. (17)) at a disc electrode of radius  $r_d = 50 \mu\text{m}$ , with a pulse amplitude  $|\Delta E| = 50 \text{ mV}$  and for different values of the difference between the formal potentials of both electrochemical steps:  $\Delta E^0 = E_2^{0'} - E_1^{0'}$ . In all cases, ADDPV curves has a centre of symmetry at the crossing potential,  $E_{cc}$ , which coincides with the average value of the formal potentials:

$$E_{cc} = \frac{E_1^{0'} + E_2^{0'}}{2} \tag{19}$$

So, the determination of this point assists the accurate extraction of the formal potentials. Besides being easier to measure than the potential or width of a peak, the  $E_{cc}$  value is independent of the pulse amplitude, the electrode size and shape, and the difference between the formal potentials ( $\Delta E^0$ ), such that this diagnosis criterion is very general.

For the  $\Delta E^0$  values considered in Figure 2.A, ADDPV curves show two peaks (a maximum and a minimum) of the same height that increases with  $\Delta E^0$  until reaching a maximum value for  $\Delta E^0 \geq 200 \text{ mV}$  corresponding to a simple E process of two electrons (see [28,35]). The  $E_{cc}$  value, and so the position of the wave, moves continuously towards more positive potentials as  $\Delta E^0$  increases. For the case  $\Delta E^0 = -35.6 \text{ mV}$ , corresponding to “non-interacting centres” [30], the shape of the ADDPV curve is the same as that of single-centre molecules although the peak current is double, as occurs in any other voltammetric technique [25-27,30].

For more negative  $\Delta E^0$  values ( $\Delta E^0 \leq -100 \text{ mV}$  in the conditions considered in Figure 2.B) the ADDPV voltammogram splits into two as the stability of the intermediate species  $O_2$  increases. As a result, four peaks (two maxima and two minima) and three crossing potentials ( $E_{c1}, E_{cc}$  and  $E_{c2}$ ) can be identified. Expressions for the values of  $E_{c1}, E_{cc}$  and  $E_{c2}$  are obtained from Eq. (17) by finding the roots of the equation for the ADDPV current:

$$\left. \begin{aligned} E_{cc} &= \frac{E_1^{0'} + E_2^{0'}}{2} \\ E_{c1} &= E_1^{0'} + \frac{RT}{F} \ln \left( \frac{-K + \frac{\Delta J}{2} + \sqrt{f(K, \Delta J)} - K\Delta J^2 - 2K\Delta J}{\Delta J} \right) \\ E_{c2} &= E_1^{0'} + \frac{RT}{F} \ln \left( \frac{-2K + \Delta J - \sqrt{f(K, \Delta J)} - 2K\Delta J^2 - 4K\Delta J}{2\Delta J} \right) \end{aligned} \right\} \tag{20}$$

with:

$$f(K, \Delta J) = 4K^2 \Delta J^4 + 16K^2 \Delta J^3 + 24K^2 \Delta J^2 + 16K^2 \Delta J + 4K^2 + \Delta J^2 - 4K \Delta J^3 - 12K \Delta J^2 - 4K \Delta J \quad (21)$$

$$\Delta J = \exp\left(\frac{F|\Delta E|}{RT}\right) \quad (22)$$

Unlike the  $E_{cc}$  value, the extreme crossing potentials  $E_{c1}$  and  $E_{c2}$  do depend on the difference between the formal potentials (through  $K$ ) and the pulse amplitude employed (through  $\Delta J$ ) in such a way that they move away when  $K$  decreases. The influence of the pulse amplitude will be discussed below (Figure 3).

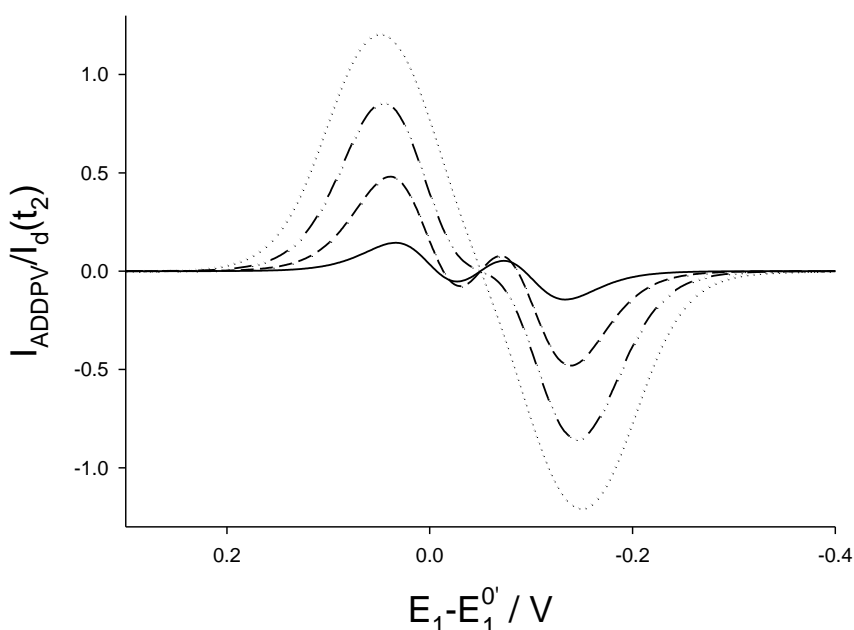


**Figure 3.** Influence of the pulse amplitude  $\Delta E$  on the dimensionless ADDPV curves for a reversible EE mechanism (Eq. (17)) at a disc electrode of radius  $r_d = 10 \mu\text{m}$ . The values of  $|\Delta E|$  (in mV) are: 25 (solid line); 50 (dashed line); 75 (dashed dotted line); 100 (dotted line).  $\Delta E^0 = -100 \text{ mV}$ . Other conditions as in Figure 2.

When the ADDPV curve shows three crossing points, the values of the formal potentials can be easily and accurately extracted from the analysis of the  $E_{c1}$ ,  $E_{cc}$  and  $E_{c2}$  values. For very negative values of  $\Delta E^0$  the determination is immediate since two well resolved waves are obtained with the characteristics of the ADDPV voltammograms of one-electron reversible processes. Thus, the extreme potentials coincide with the corresponding formal potentials:  $E_{c1}(K \rightarrow 0) \rightarrow E_1^{0'}$  and  $E_{c2}(K \rightarrow 0) \rightarrow E_2^{0'}$ .

The splitting of the ADDPV signal (i.e., the number of real roots of Eq. (17)) depends on the value of the pulse amplitude (see Eq. (20)). In Figure 3 the influence of  $\Delta E$  on the ADDPV curves is plotted for the EE mechanism with  $\Delta E^0 = -100 \text{ mV}$  at a disc microelectrode of radius  $r_d = 10 \mu\text{m}$ . For a given  $\Delta E^0$  value, the separation of the peaks is promoted by the use of small values of the pulse

amplitude. Thus, only two peaks are observed in Figure 3 for large  $|\Delta E|$  values, whereas four peaks and three crossing potentials can be obtained by decreasing  $|\Delta E|$ . The use of small  $\Delta E$  values has other beneficial effects like the reduction of charging current effects and the obtaining of better defined (less broad) peaks, although the magnitude of the signal is smaller.

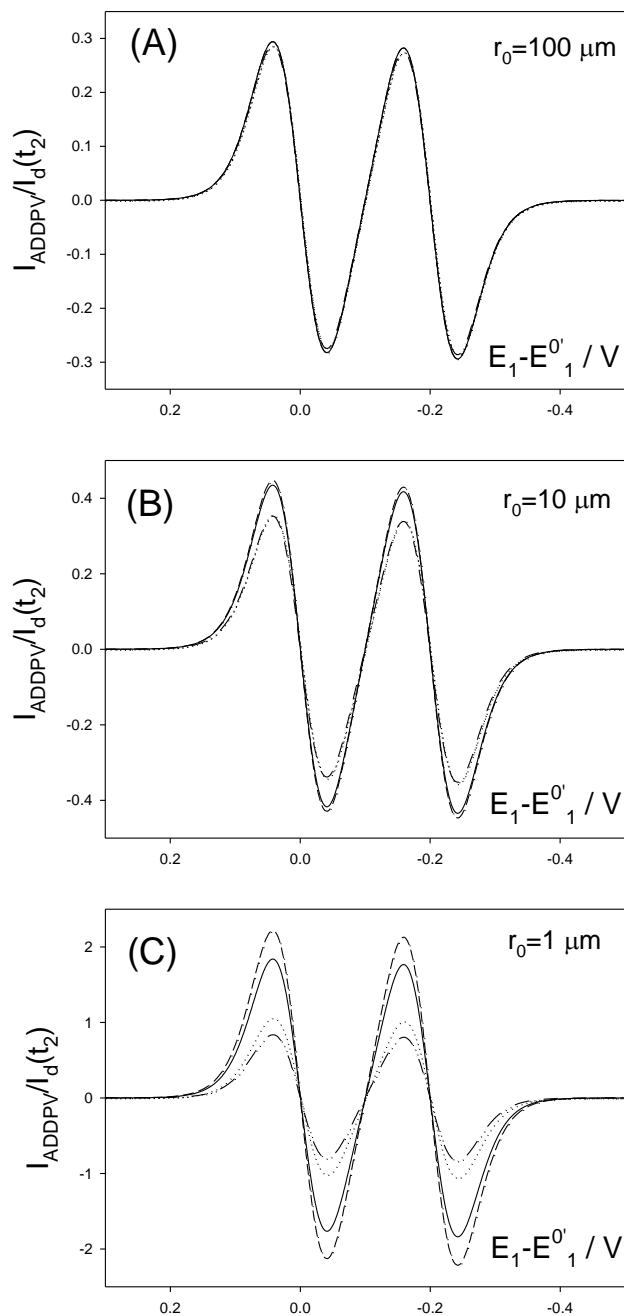


**Figure 4.** Dimensionless ADDPV curves (Eq. (17)) for a reversible EE mechanism calculated for spherical (solid lines), disc (dashed lines), cylindrical (dashed dotted lines) and band (dotted lines) electrodes of different sizes. The values of  $r_0$  ( $=r_d = r_s = (w/2) = r_c$ ) (in  $\mu\text{m}$ ) are indicated on the curves.  $|\Delta E| = 50 \text{ mV}$ ,  $\Delta E^0 = -200 \text{ mV}$ . Other conditions as in Figure 2.

From the equations deduced in section 2, the limiting value of  $\Delta E^0$  to obtain three crossing potentials has been calculated by considering that the differences between the extreme crossing potentials,  $E_{c1}$  and  $E_{c2}$ , and the central crossing potential,  $E_{cc}$ , should be greater than 4 mV. For the typical value  $|\Delta E|=50$  mV  $E_{c1}$ ,  $E_{c2}$  and  $E_{cc}$  are well defined for  $\Delta E^0 \leq -85$  mV. This value increases with the pulse amplitude such as for  $|\Delta E|=75$  mV four peaks are obtained for  $\Delta E^0 \leq -105$  mV. Note that, as discussed above, the central crossing potential is not affected by this parameter in agreement with Eq. (19).

The effect of the electrode size and shape on the ADDPV curves is analyzed in Figure 4 for the EE mechanism with  $\Delta E^0 = -200$  mV (four peaks, two well separate processes) at discs, spheres, bands and cylinders with a characteristic dimension  $r_0$  ( $= r_d = r_s = (w/2) = r_c$ ). The voltammograms obtained at different electrode geometries are coincident for  $r_0 = 100$   $\mu\text{m}$  (Figure 4.A) since for this size the prevalent diffusion field is planar, in such a way that the electrode geometry becomes irrelevant (see Table 1). As the electrode size is decreased (Figures 4.B and 4.C), the temporal dependence of the response diminishes and the divergences between the ADDPV curves of different electrode geometries increase. Finally, the response reaches a steady state (disc, sphere) or quasi-steady state (band, cylinder) behaviour (Figure 4.C). Under these conditions, the ratio between the ADDPV currents at discs and spheres of equal radius  $r_d = r_s$  is given by:

$$\frac{I_{ADDPV, disc}^{ss}}{I_{ADDPV, sphere}^{ss}} = \frac{1}{\pi} \quad (23)$$

in agreement with Eq. (17) and expressions in Table 1.

In the case of cylinder and band electrodes a stationary response cannot be attained [34], but it is also possible to find an equivalence relationship between them at a fixed time value when the characteristic dimensions of both electrodes fulfil  $r_c = w/4$ :

$$\frac{I_{ADDPV, band}}{I_{ADDPV, hemicylinder}} = 1 \quad (24)$$

It is worth highlighting that in any case the crossing potentials do not depend on the electrode shape and size since they are obtained from the potential function  $(\Omega_{2,n} + \Omega_{2,r})$  which is independent of the particular electrode geometry.

In resume, the shape of the ADDPV response of an EE mechanism only depends on the difference between the formal potential of the electron transfers and the pulse amplitude employed. When four peaks are recorded, the values of the formal potentials of both steps can be extracted from the values of the crossing potentials. When only two peaks are obtained, the simultaneous analysis of the values of the crossing potential and the peak current or width is required for the extraction of  $E_2^{0'}$  and  $E_1^{0'}$ .

With this purpose the variation of the dimensionless peak current and width with  $\Delta E^0$  are given in Figure 5 for the four geometries considered in this paper. Since the ADDPV response is symmetrical, we will only discuss the behaviour of the parameters of the maximum.

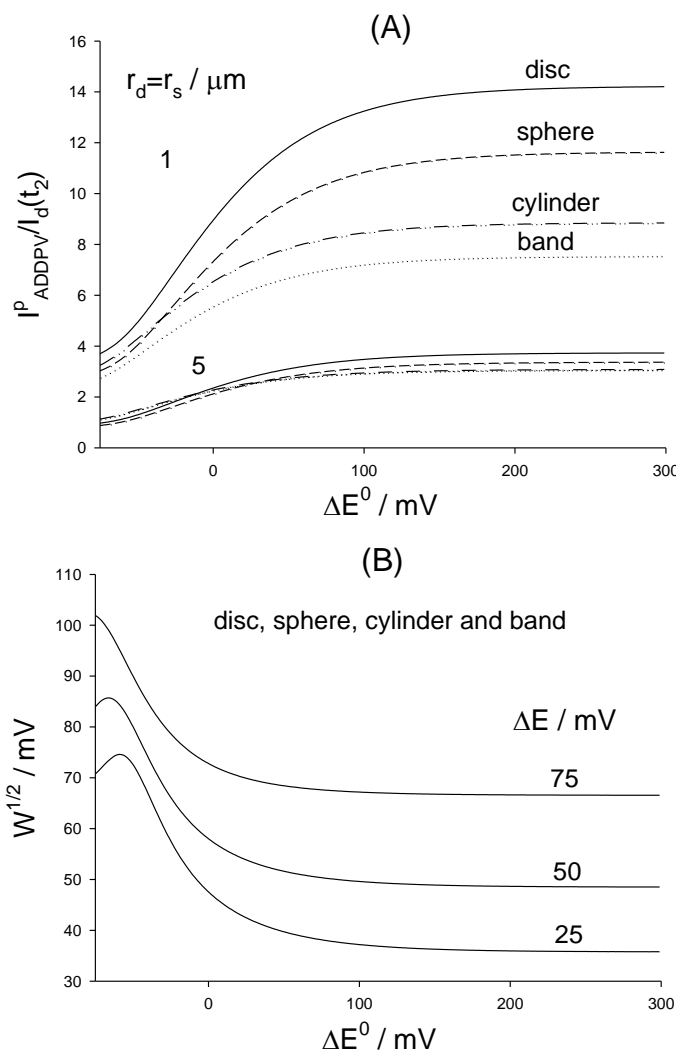


**Figure 5.** Evolution of the ADDPV maximum / minimum dimensionless peak height (A) and of the half peak width (B) with  $\Delta E^0$  for a reversible EE mechanism calculated for spherical (solid lines), disc (dashed lines), cylindrical (dashed dotted lines) and band (dotted lines) electrodes of different sizes with  $|\Delta E| = 50 \text{ mV}$  (A) and for three values of the pulse amplitude (in mV) (B). Other conditions as in Figure 2.

As can be seen in Figure 5.A, the maximum peak height increases with  $\Delta E^0$  until reaching the value corresponding to an E process of two electrons for  $\Delta E^0 > 150 \text{ mV}$ . The differences between the value of the peak height at different geometries are more apparent as the electrode size decreases, as was previously shown in Figure 4.

Other interesting parameter is the half-peak width,  $W^{1/2}$ , which varies with  $\Delta E^0$  according to Figure 5.B. One of the advantages of employing this parameter is that the  $W^{1/2}$ -value does not depend

on the electrode geometry and other experimental variables (e.g., concentration of the electroactive species, diffusion coefficient), unlike the peak height. The half-peak width is only dependent on  $\Delta E^0$  for a given pulse amplitude and it decreases as the  $\Delta E^0$ -value increases up to the value associated with an E process of two electrons for  $\Delta E^0 > 150$  mV (which corresponds to  $W^{1/2} = 48$  mV for the typical value  $\Delta E = 50$  mV). Note also that the use of large pulse amplitudes causes a great broadening of the peaks. Thus, for example, for  $\Delta E^0 = 100$  mV the half-peak width varies from 37 mV for  $\Delta E = 25$  mV to 67 mV for  $\Delta E = 75$  mV.

#### 4. CONCLUSIONS

Easy-to-manage, analytical expressions have been derived for the study of reversible multiple electron transfer reactions by additive differential double pulse voltammetry (ADDPV). The theory presented is valid for any number of electrochemical steps, any difference between the formal potentials of the various redox couples and any size of the electrode, covering the geometries most commonly employed in electrochemical experiments: discs, (hemi)spheres, bands and cylinders.

The case of a two-electron reducible molecule (EE mechanism) has been analyzed showing the variation of the ADPPV curves with the difference between the formal potentials,  $\Delta E^0 = E_2^{0'} - E_1^{0'}$ , the electrode size and the pulse amplitude. The technique has the advantage that by decreasing the value of the pulse amplitude ( $|\Delta E|$ ) the characteristic behaviour of an EE mechanism of four peaks and three crossing potentials ( $E_{cc}$ ,  $E_{c1}$  and  $E_{c2}$ ) can be achieved even for some high  $\Delta E^0$ - values. This facilitates the extraction of the formal potentials.

In all cases, the central crossing potential ( $E_{cc}$ ) is a symmetry point and its value is equal to the average value of the formal potentials (independently of any experimental variable). When three crossing points are available, the extraction of  $E_1^{0'}$  and  $E_2^{0'}$  can be carried out from the  $E_{cc}$ ,  $E_{c1}$  and  $E_{c2}$  values that can be measured with very good precision. When the ADPPV curve shows only one intercept, the values of the height or width of the peaks together with the crossing potential enable the determination of the two formal potentials.

#### ACKNOWLEDGEMENTS

A. M. and J. G. greatly appreciate the financial support provided by the Dirección General de Investigación Científica y Técnica (Project Number CTQ2009-13023), and the Fundación SENECA (Project Number 08813/PI/08). E. L. thanks the Fundación SENECA for the grant received.

#### References

1. S. Barlow and D. O'Hare, *Chem. Rev.*, 97 (1997) 637-669.
2. F. Barrière and W. E. Geiger, *J. Am. Chem. Soc.*, 128 (2006) 3980-3989.
3. E. Hillard, F. De Abreu, D. C. M. Ferreira, G. Jaouen, M. O. F. Goulart and C. Amatore, *Chem. Comm.*, (2008) 2612-2628.
4. D. H. Evans, *Chem. Rev.*, 108 (2008) 2113-2144.

5. S. C. B. Oliveira and A. M. Oliveira-Brett, *J. Electroanal. Chem.*, 648 (2010) 60–66.
6. E. Palecek, *Anal. Biochem.*, 170 (1988) 421–431.
7. D. Bruns, *Methods*, 33 (2004) 312–321.
8. R. Sardar, A. M. Funston, P. Mulvaney and R. W. Murray, *Langmuir*, 25 (2009) 13840-13851.
9. F. Barrière and W. E. Geiger, *J. Am. Chem. Soc.*, 128 (2008) 3980-3989.
10. J. B. Flanagan, S. Margel, A. J. Bard and F. C. Anson, *J. Am. Chem. Soc.*, 100 (1978) 4248-4253.
11. Z. Rongfeng and D. H. Evans, *J. Electroanal. Chem.*, 385 (1995) 201-207.
12. D. H. Evans and M. W. Lehmann, *Acta Chem. Scand.*, 53 (1999) 765-774.
13. A. Molina, C. Serna, M. López-Tenés and M. M. Moreno, *J. Electroanal. Chem.*, 576 (2005) 9-19.
14. D. S. Polcyn and I. Shain, *Anal. Chem.*, 38 (1966) 370-375.
15. R. L. Myers and I. Shain, *Anal. Chem.*, 41 (1969) 980-989.
16. C. P. Andrieux and J. M. Savéant, *J. Electroanal. Chem.*, 28 (1970) 339-348.
17. D. E. Richardson and H. Taube, *Inorg. Chem.*, 20 (1981) 1278-1285.
18. C. Amatore, M. F. Bento and M. I. Montenegro, *Anal. Chem.* 67 (1995) 2800-2811.
19. M. W. Lehmann and D.H. Evans, *Anal. Chem.*, 71 (1999) 1947-1950.
20. A. Molina, C. Serna, M. López-Tenés and R. Chicón, *Electrochem. Comm.*, 2 (2000) 267-271.
21. A. Molina, M. M. Moreno, C. Serna, M. López-Tenés, J. González and N. Abenza, *J. Phys. Chem. C*, 111 (2007) 12446-12453.
22. M. López-Tenés, A. Molina, C. Serna, M. M. Moreno and J. González, *J. Electroanal. Chem.*, 603 (2007) 249-259.
23. S. R. Belding, J. G. Limon-Petersen, E. J. F. Dickinson and R. G. Compton, *Angew. Chem. Int. Ed.*, 49 (2010) 9242-9245.
24. S. Komorsky-Lovric and M. Lovric, *J. Electroanal. Chem.*, 660 (2011) 22–25.
25. A. Molina, J. González, E. Laborda, Q. Li, C. Batchelor-McAuley and R. G. Compton, *J. Phys. Chem. C*, 116 (2012) 1070-1079.
26. E. Laborda, A. Molina, Q. Li, C. Batchelor-McAuley and R. G. Compton, *Phys. Chem. Chem. Phys.*, (2012) DOI: 10.1039/C2CP40265C.
27. A. Molina, C. Serna, Q. Li, E. Laborda, C. Batchelor-McAuley and R. G. Compton, *J. Phys. Chem. C*, (2012) DOI: 10.1021/jp302075t.
28. A. Molina, M. M. Moreno, C. Serna and L. Camacho, *Electrochem. Comm.*, 3 (2001) 324-329.
29. C. Serna, A. Molina, M. M. Moreno and M. López-Tenés, *J. Electroanal. Chem.*, 546 (2003) 97-108.
30. A.J. Bard and L. Faulkner, *Electrochemical Methods: Fundamentals and Applications*, 2nd Ed., Wiley & Sons, New York, 2001.
31. D. Shoup and A. Zsabo, *J. Electroanal. Chem.*, 140 (1982) 237–245.
32. A. Zsabo, D. K. Cope, D. E. Tallman, P. M. Kovach and R. M. Wightman, *J. Electroanal. Chem.*, 217 (1987) 417–423.
33. K. Aoki, K. Tokuda and H. Matsuda, *J. Electroanal. Chem.*, 225 (1987) 19–32.
34. A. Molina, J. González, M. Henstridge and R. G. Compton, *J. Phys. Chem. C*, 115 (2011) 4054-4062.
35. A. Molina, M. M. Moreno, M. López-Tenés and C. Serna, *Electrochem. Comm.*, 4 (2002) 457-461.